Numerical Analysis of Ballistic Impact Damage in Layered Isotropic Plates

I. Smojver[a], F. Lukač[b] and D. Ivančević[a]

[a]Department of Aeronautical Engineering, Faculty of Mechanical Engineering and Naval Architecture, University of Zagreb

I. Lučića 5, HR-10000, Zagreb, Croatia

[b]Đuro Đaković Special Vehicles

Dr. Mile Budaka 1, Slavonski Brod, Croatia

Abstract*: The work presents a numerical procedure employed for the simulation of high-velocity impact phenomena at Weldox 460 E steel plates. Parameters which affect the plate impact resistance have been analyzed in this work. These include projectile nose shape, impact velocity and incidence angle, and the target plate thickness and configuration. The impact velocities are in the range of 75 to 550 m/s, whereas the mass of the impactor is approximately 0.2 kg. The thickness of the stationary target plates has been varied from 10 to 20 mm.*

The simulations have been performed in Abaqus/Explicit as to apply the broad range of available material models and due to the robustness of the simulation in highly nonlinear transient problems, where complex contact conditions are present. The Johnson-Cook strain rate dependent plasticity model has been implemented to realistically simulate the impact behavior of the target plate. Additionally, a Continuum Damage Mechanics model has been employed as to model the damage processes in the material. According to this model, damage effects are triggered based on the value of equivalent plastic strain in the material. Plate perforation has been simulated using the element deletion criterion based on the damage parameter.

The material parameters of the constitutive model have been determined from the literature and by validation against the experimental ballistic curves available in the literature. The numerical simulations have correctly replicated the available experimental results, thereby confirming the validity of the numerical procedure and the utilized material constitutive laws, as well as degradation and failure models.

Keywords*: Ballistic impact, High-velocity impact, Ballistic limit, Strain rate effects, Impact behavior.*

1. Introduction

A large number of parameters which affect the ballistic performance of the armor protection have to be evaluated to determine the optimal set of design characteristics for the best level of ballistic protection. Numerical methods are in this process an important asset, as the scope and amount of experimental testing can be significantly reduced. This work presents results of a preliminary research performed as part of a project proposal aimed at the numerical simulation of advanced protective structures.

Ballistic perforation is a highly nonlinear phenomenon that includes the interaction of several aspects which all have to be realistically considered by the numerical model, as to achieve reliable results. These include the strain-rate dependent material behavior of the impacted target and the impactor, temperature effects, complex contact conditions, and the material fracture and failure models. In order to account for all these phenomena, the Johnson-Cook strain rate and temperature dependent constitutive model has been employed to realistically simulate the target plate during the high velocity perforation. In addition, application of an appropriate constitutive model for the impactor results in the physically accurate modelling of the impact.

The constitutive model is one of the critical components of the numerical model which affect the compliance with experimental results, as highlighted in the literature, e.g. in (Børvik, 2000), (Ali, 2009), (Arias, 2008). One of the most widely employed constitutive models for the ballistic impact problems is the Johnson-Cook plasticity model (Johnson, 1983). The model includes the effects of plastic strain, strain rate and temperature and has been applied in e.g. (Arias, 2008), (Kiliç, 2013), (Shánĕl, 2014), (Jankowiak, 2013). One of the main deficiencies of the original Johnson-Cook model is that the effects of strain rate and temperature are not interrelated, as stated in (He, 2013).

In order to increase the fidelity of the numerical results, modified versions of the Johnson-Cook plasticity model have been exploited, as e.g. in (Børvik, 2000). These models account for the interrelation of the strain rate and temperature effects. Additionally, damage initiation and propagation laws are employed in the models to simulate the material fracture caused by the penetration of the impactor (Børvik, 2000). The numerical framework described in this work exploits the comprehensive numerical capabilities of Abaqus/Explicit. Therefore, only the built-in constitutive models have been implemented in this work, whereas user-defined constitutive modelling is planned to be used in the continuation of the research.

2. Numerical framework

The numerical framework utilized for the analyzed problem is shown in Figure 1. The experimental results provided in (Børvik, 2000) have been used for the validation of the numerical framework. The experimental data have been obtained in gas-gun testing using blunt, conical and hemispheric tip shapes. The 6 – 30 mm thick target plates have been tested in the velocity range of 75 – 450 m/s.

The boundary conditions in the numerical model have been defined as to replicate the experimental setup. in which the target plates have been fixed using 21 bolts located at a diameter of 550 mm. The plate is fixed to a rigid frame which has a 500 mm diameter opening which enables deflection of the plate. These conditions have been simulated by modelling only the part of the plate which can be deformed. Consequently, the numerical model of the target plate has a circular shape with the diameter of 500 mm. All displacement degrees of freedom of the nodes located at the outer plate diameter have been restricted as to replicate the boundary conditions of the experimental setup. The plate thickness has been varied as to simulate impacts on target plates with various thicknesses made from Weldox 460 E steel. The plate is impacted at the center by the impactor made from Arne tool steel.

The initial velocity has been varied to obtain the numerical results which have been compared to the experimental ones. The experimentally observed properties are the ballistic limit (the lowest velocity which results in the penetration of the plate) and the ballistic curves which define the correlation of the initial velocity and the residual velocity of the impactor after the plate perforation. The ballistic curves are particularly important for the validation of the numerical model as they enable insight into the accuracy of the employed constitutive models for the correct simulation of the plate and impactor ballistic behavior.

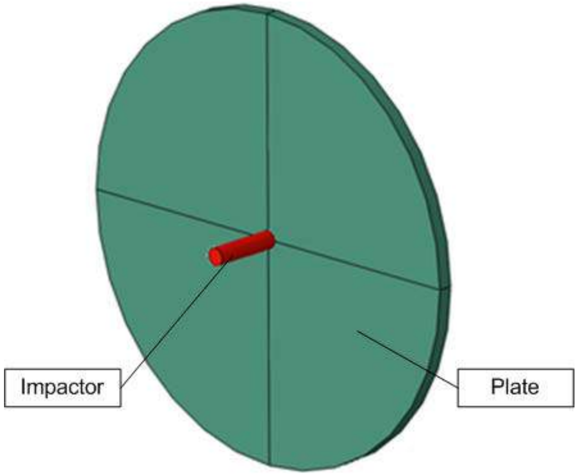

Figure 1.Numerical setup of the analyzed impact problem.

2.1 Numerical model of the impacted plate

The targeted plate has been discretized using the hexahedral C3D8R finite elements to avoid possible problems caused by the shear locking. The plate finite element model has been shown in the Figure 2. The discretization level of the targeted plate finite element mesh has been selected as a compromise between the computational effectiveness and the accuracy of the simulation.

The finite element mesh has been refined at the center as to more accurately capture the stress distribution at the impact location. Therefore, these elements have the typical element length of approximately 0.3 mm, whereas element sizes of approximately 10 mm have been employed for discretization of the parts of the plate which are distant from the impact location, in order to enhance the computational effectiveness. The reasonably coarse mesh causes relatively distorted finite elements in some parts of the numerical model. However, the distorted finite elements are not present at the impact location, as shown in Figure 2. The typical through thickness discretization is shown in the right-hand side image in Figure 2. The number of finite elements in the numerical model depends approximately linearly on the plate thickness. The number of finite elements and nodes in the numerical models of the analyzed plates is shown in Table 1.

Table 1.Details of the plate numerical models.

Plate thickness	Number of C3D8R elements	Number of nodes
10 mm	291100	307776
12 mm	349320	366400
16 mm	465760	483648
20 mm	582200	600896
24 mm	698640	718144

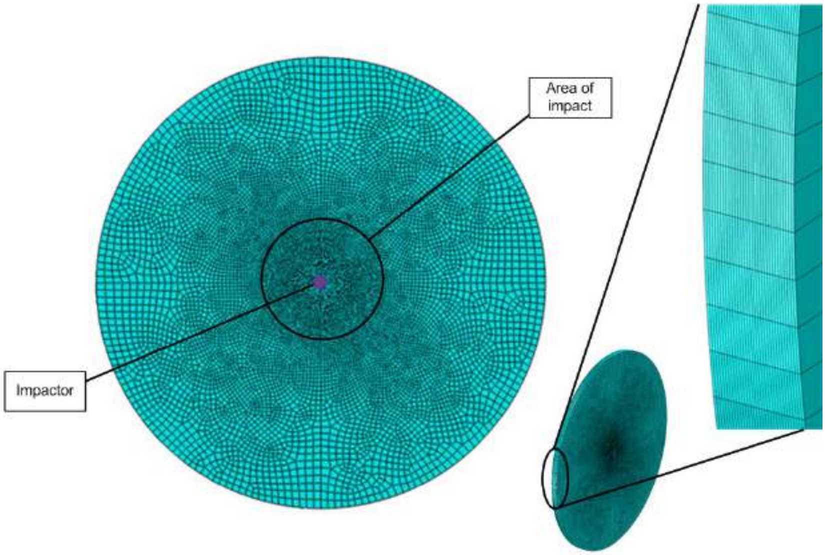

Figure 2.Finite element model of the target plate.

The constitutive model employed in this work for the target plate is the Abaqus built-in Johnson-Cook strain rate plasticity model (Abaqus User's Manual). The parameters of the numerical model have been selected to realistically simulate the experimental data for the blunt impact testing provided in (Børvik, 2000). The constitutive model is isotropic elastic, whereas the nonlinear behavior has been captured by the Johnson-Cook plasticity model which defines the rate dependent yield stress as

$$\bar{\sigma} = \left[A + B \cdot \varepsilon_{pl}^{n} \right] \cdot \left[1 + C \ln \frac{\dot{\bar{\varepsilon}}_{pl}}{\dot{\varepsilon}_0} \right] \cdot \left[1 - \left(\frac{T - T_0}{T_{melt} - T_0} \right)^m \right]. \quad (1)$$

In Equation (1), A is the static yield stress, B and n are the strain hardening parameters, C is the material parameter which defines the strain rate effects and m is the parameter which accounts for the temperature dependent softening of the material (Abaqus User's Manual). T_{melt} in Equation (1) is the melting temperature of the material, whereas T_0 is the transition temperature below which the yield stress is independent on the temperature. Finally, $\dot{\varepsilon}_0$ is the material referent strain rate, while $\dot{\bar{\varepsilon}}_{pl}$ is the equivalent plastic strain rate.

The Johnson-Cook dynamic failure model has been employed for modelling of the failure process in the material. According to this model, material failure is modelled when the damage parameter, calculated as

$$\omega = \sum \frac{\Delta \bar{\varepsilon}_{pl}}{\varepsilon_{pl}^{f}}, \quad (2)$$

exceeds the value of one. $\Delta\varepsilon_{pl}$ in Equation (2) is the increment of the equivalent plastic strain, whereas the strain at failure ε_{pl}^{f} is defined as

$$\varepsilon_{pl}^{f} = \left[D_1 + D_2 \exp\left(D_3 \frac{p}{q} \right) \right] \cdot \left[1 + D_4 \ln \frac{\dot{\bar{\varepsilon}}_{pl}}{\dot{\varepsilon}_0} \right] \cdot \left[1 + D_5 \frac{T - T_0}{T_{melt} - T_0} \right]. \quad (3)$$

The parameters $D_1 - D_5$ in Equation (3) are material parameters which determine the material failure process, *p* is the pressure stress and *q* is the von Mises stress (Abaqus User's Manual).

The material model assumes that the impact is an adiabatic event. Consequently, the heat generated by the plastic deformation cannot be interchanged between the impacting bodies - a reasonable assumption for the rapid event analyzed in this work. According to the constitutive model, the temperature rate is defined using the empiric relation

$$\dot{T} = \chi \frac{\boldsymbol{\sigma} : \dot{\boldsymbol{\varepsilon}}_{pl}}{\rho c(T)}, \quad (4)$$

where χ is the inelastic heat fraction, ρ is the density and *c* is the temperature dependent specific heat. The employed mechanical properties for this material are provided in Table 2. These parameters have been taken from (Børvik, 2000). The damage parameters for the Johnson-Cook model of the impacted plate have been modified to replicate the experimental results, with higher accuracy in a wide range of initial impactor velocities.

Table 2. Weldox 460 E mechanical properties and parameters of the Johnson-Cook plasticity model, after (Børvik, 2000).

E [GPa]	ν [−]	χ [−]	$c[J/K]$	$\rho[\mathrm{kg/m^3}]$	$T_{melt}[K]$	$T_0[K]$
200	0.33	0.9	452	7850	1800	293
$A[MPa]$	$B[MPa]$	$n[-]$	$C[-]$	$m[-]$	$\dot{\varepsilon}_0[s^{-1}]$	
490	807	0.73	0.012	0.94	$5 \cdot 10^{-4}$	
$D_1[-]$	$D_2[-]$	$D_3[-]$	$D_4[-]$	$D_5[-]$		
0.0705	1.732	-0.54	-0.0123	0		

2.2 Numerical model of the impactor

The impactor has been made from the Arne tool steel with the properties provided in Table 3, as defined in (Børvik, 2000). Two impactor material models have been implemented in the simulations - the isotropic elastic model and the linearly isotropic plasticity model. The element removal criterion based on the value of the equivalent plastic strain has been additionally utilized in the simulations with the plasticity material model. The two impactor shapes modeled in this work are shown in Figure 3. The blunt impactor's finite element model has been discretized using 35520 C3D8R elements, whereas 13908 C3D8R elements have been employed for the impactor with the conical tip shape.

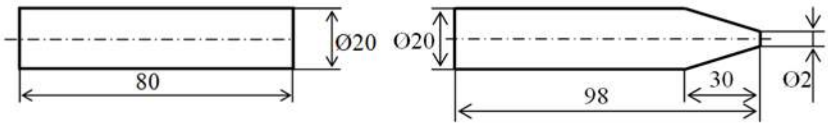

Figure 3.Impactor shapes, dimensions in [mm].

Table 3. Arne tool steel mechanical properties (Børvik, 2000).

E [GPa]	σ_y [MPa]	E_p [GPa]	ν [-]	ε_f [-]	ρ [kg/m^3]
204	1900	15.0	0.33	0.0215	7850

3. Analysis

The general contact algorithm in Abqaus/Explicit has been exploited to model the contact between the plate and the impactor. This algorithm allows modelling of the contact between the external plate and impactor surfaces, as well as with the internal surfaces which are generated after the removal of failed finite elements throughout the plate perforation process. The friction has been included in the contact algorithm by using a constant friction coefficient of 0.15.

4. Results

4.1 Validation of the numerical model

The initial velocity vector of the impactor has been defined to be normal to the target plate in the analyses used in the validation of the numerical model. The experimental ballistic curves provided in (Børvik, 2000) have been used for the validation of the numerical model. Therefore, the initial impactor velocity has in the simulations been varied as to obtain the impactor residual velocities which have been compared to the available experimental data. Initially, the plasticity has been neglected for the impactor material.

The stress distribution at five time frames during the blunt impact with the initial velocity of 338 m/s at the 20 mm target plate is shown in Figure 4. The physical behavior of the plate during the impact event, which results in the formation of the shear plug, has been captured correctly as shown in this Figure.

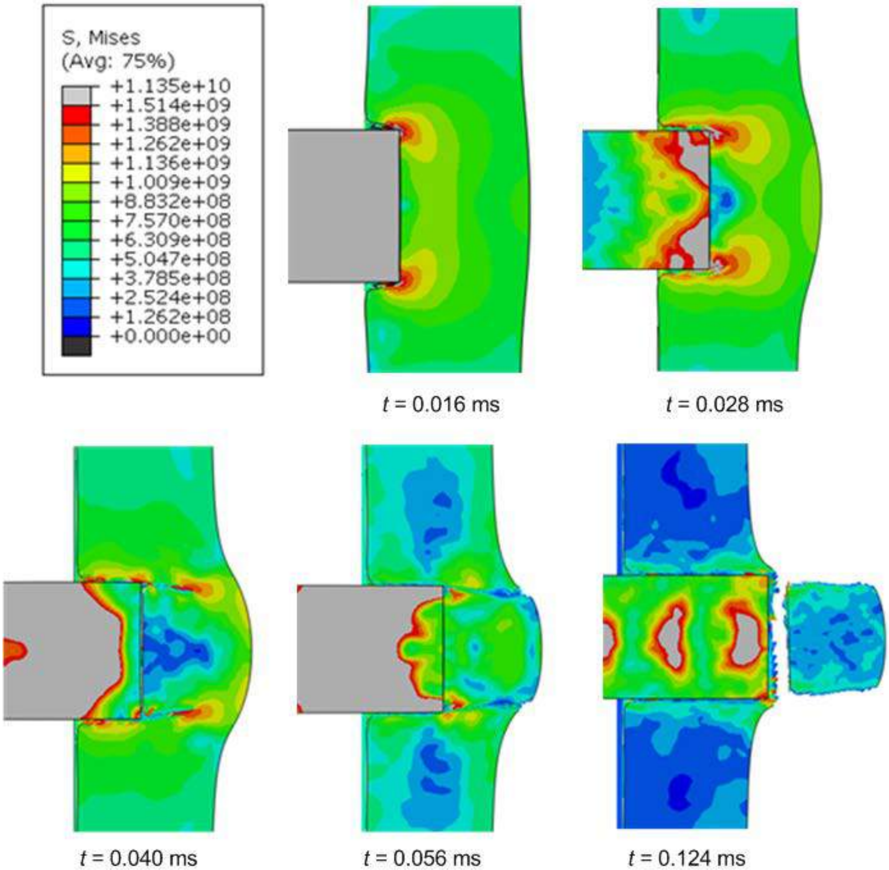

Figure 4.Von Mises stress distribution in [Pa] at the perforation of a 20 mm plate impacted by the elastic impactor at 338 m/s.

The comparison of the numerically predicted and experimentally measured ballistic curves is shown in Figure 5. These curves have been obtained by interpolation of the residual velocities for four target plate thicknesses (10, 12, 16 and 20 mm). The results shown in this Figure have been calculated using the ideally elastic material model for the impactor. The initial impact velocities in the simulations have been set equal to the relevant velocities in the experiments provided in (Børvik, 2000). Additionally, several simulations have been performed in the velocity range close to the numerically predicted ballistic limit, as to determine this value with a higher accuracy.

An average number of 30 simulations have been performed to obtain the ballistic curves shown in Figure 5. The analyzed time periods in the simulations have been between 0.4 ms – 0.8 ms. The higher analyzed time periods were necessary for the simulations with the velocity closer to the ballistic limit, since the slowing down and bouncing of the projectile has to be simulated in these analyzes.

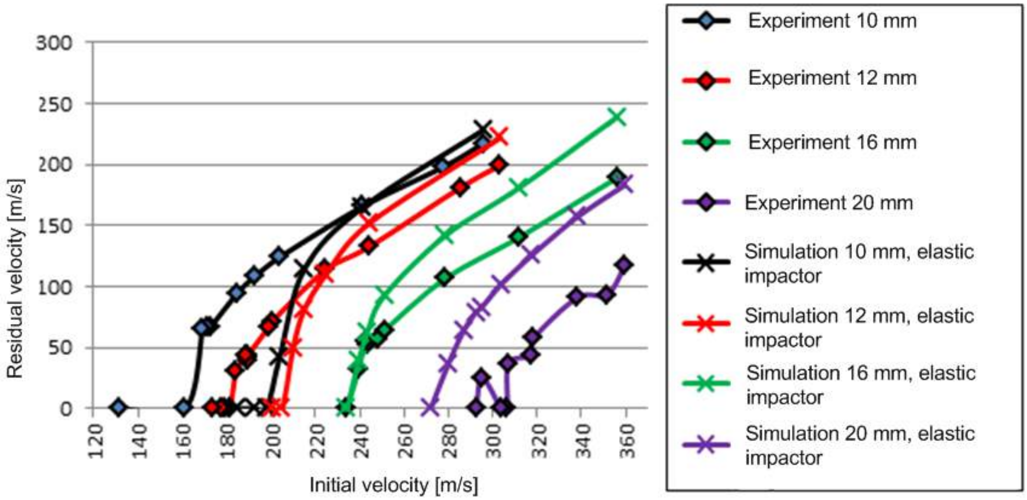

Figure 5.Comparison of numerical and experimental ballistic curves (Børvik, 2000) in the simulations with the ideally elastic impactor material model.

As shown in Figure 5, the numerical results differ from the experimentally predicted values. This difference is more pronounced with the increase of the plate thickness. Consequently, the results for the 20 mm plate show the highest discrepancy compared to the experimental results. The numerically predicted ballistic limit is in this case approximately 40 m/s lower (13%) compared to the experimentally determined value.

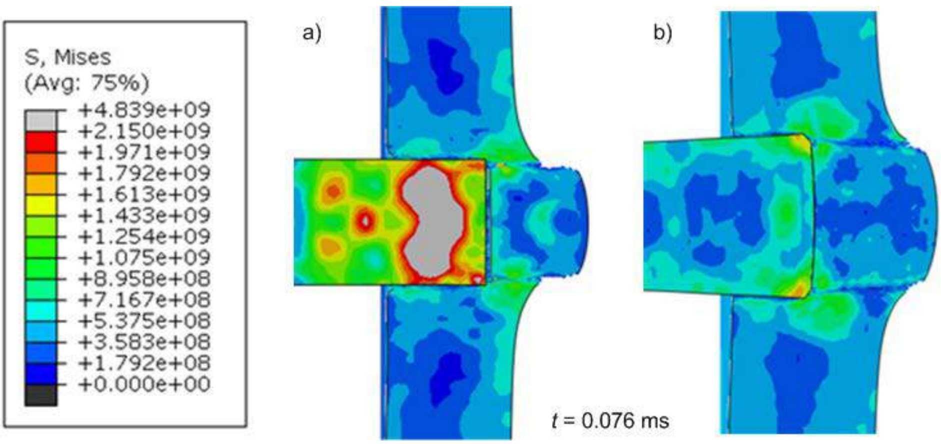

Figure 6.Comparison of blunt shaped projectile impact: a) ideally elastic impactor and b) plastic impactor. The results show the Von Mises stress distribution in [Pa].

Figure 6 shows the effect of the impactor material model at the physical behavior and stress distribution of the impacting instances with the 338 m/s impact at the 20 mm thick plate. Inclusion of the plasticity material model for the impactor resulted in a more realistic behavior of the impactor, and in an overall better matching with the experimental ballistic curves.Consequently, the rest of the results presented in this work have been calculated using the plasticity material model of the impactor. As shown in Figure 6, the plastic deformation of the impactor prior to the plate perforation leads to the increase of the effective impactor cross-section thereby additionally reducing the impactor velocity. Thus, the numerically predicted ballistic resistance of the target plates has been increased.

The physical effect of the increase in the plates' ballistic resistance is clearly demonstrated in Figure 7. As shown, the numerically calculated ballistic curves are in these simulations a much better representation of the experimental results, over the range of analyzed plate thicknesses and impact velocities. The match with the experimental results is worst for the 12 mm thick plate, where the bending deformation of the plate is most pronounced.

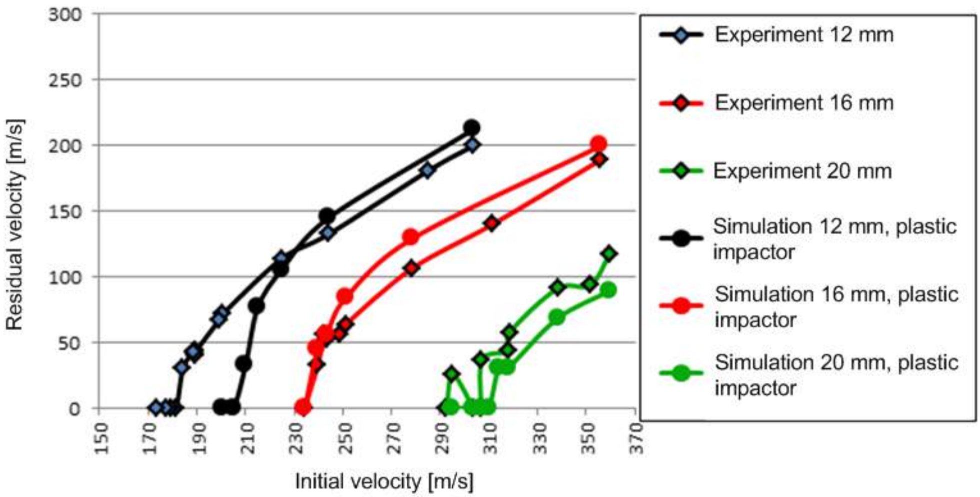

Figure 7.Comparison of numerical results, obtained with the plastic material model for the impactor, and the experimental results (Børvik, 2000).

4.2 Effect of impact incidence angle

The effect of target plate incidence angle on the ballistic resistance has been analyzed in this Section. In total, 21 simulations with the average simulated time of 1.5 ms, have been performed to evaluate the influence of the impact incidence angle. The initial layout for these simulations is shown in Figure 8. As demonstrated, the target plate incidence angle has been analyzed by the variation of impact angle and initial velocity vector of the projectile.

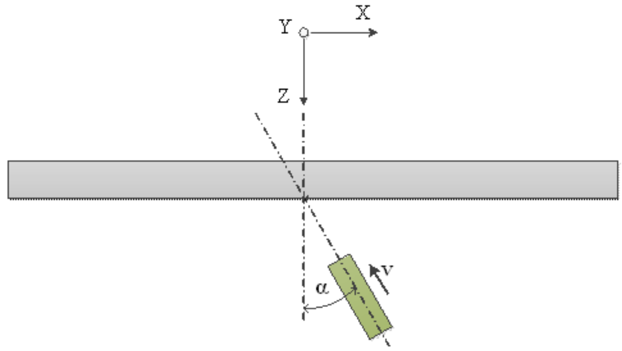

Figure 8.Effective thickness of the impacted plate.

Figure 9 illustrates the effect of target plate incidence on the ballistic curves. These simulations have been performed using the blunt impactor and the16 mm thick plate. The experimental values in this Figure are shown for the normal impact, and are taken from (Børvik, 2000). As expected, the increased effective thickness of the target plate leads to the improved ballistic resistance, which is evident in the improved ballistic limits and the general shifts of the ballistic curves to the right-hand side of the diagram with an increase of the incidence angle. As depicted in Figure 9, the ballistic limit increases by approximately 36% with the increase of the incidence angle from 0 to 20°.

The initial impact velocity of 356 m/s has been highlighted in this Figure as to illustrate the effect of the impact incidence angle for the highest initial velocity, for which the experimental values are provided in (Børvik, 2000). As shown, the residual velocity decreases by approximately 42% with the increase of the incidence angle from 0° to 20°.

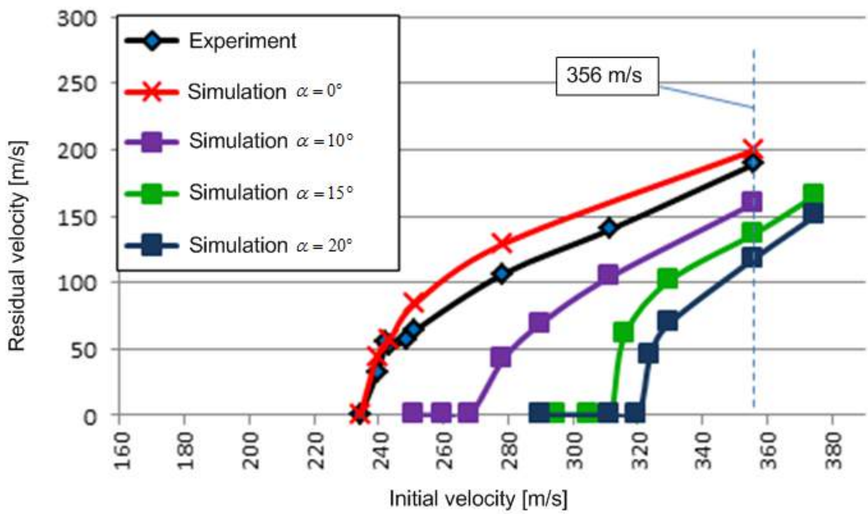

Figure 9.Ballistic curves for impacts at various incidence angles.

The inclusion of the target plate incidence results in the deflection of the projectile direction, as shown in Figure 10. The results in this Figure show the perforation of the 16 mm plate at the 20° incidence angle and the initial velocity of 330 m/s. The blunt impact at the incidence angle also results in the formation of the shear plug. As shown in Figure 10, the output velocity vector is deflected toward the normal of the impacted plate. Consequently, the incidence angle is continuously decreased during the perforation analysis. The physical interpretation of the velocity vector deflection is in the asymmetrical contact conditions which also cause the asymmetrical perforation in this impact case, as shown in Figure 10.

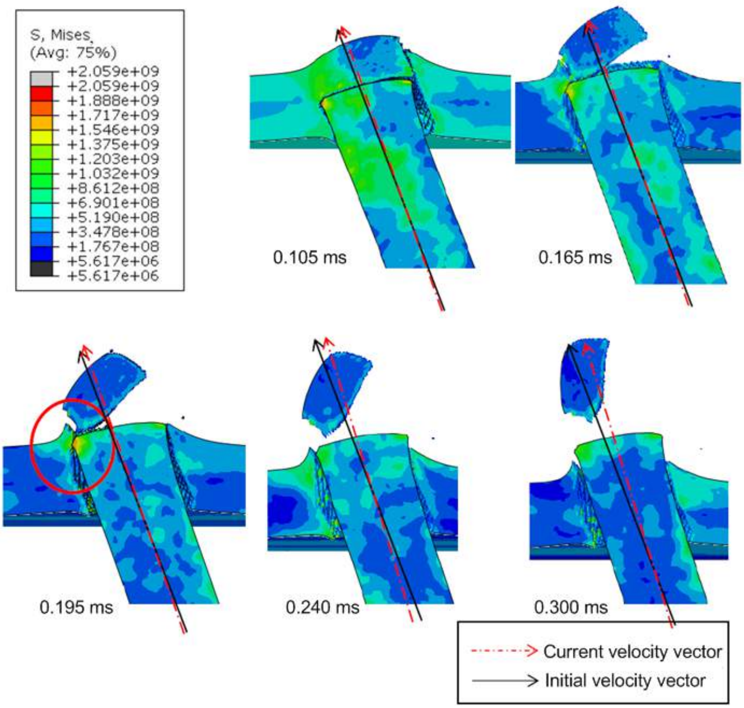

Figure 10.Von Mises stress distribution in [Pa] during the 16 mm thick plate perforation at 20° incidence angle and the 330 m/s initial velocity.

4.3 Effects of impactor shape and target configurations

The effect of the impactor tip shape has been studied numerically using the conically shaped impactor, representing the approximate shape of realistic impactors. This effect has been analyzed using the 12 mm thick plate, while the initial velocity vector has been set to be perpendicular to the target plate Simulation within time frame of 0.3 ms to 0.8 ms has been necessary to capture the perforation processes in these analyses. The stress distribution at the 300 m/s impact of the conical impactor is shown in Figure 11. The perforation process of the conically shaped impactor is fundamentally different compared to the blunt impact case, since the plug is not formed in this case.

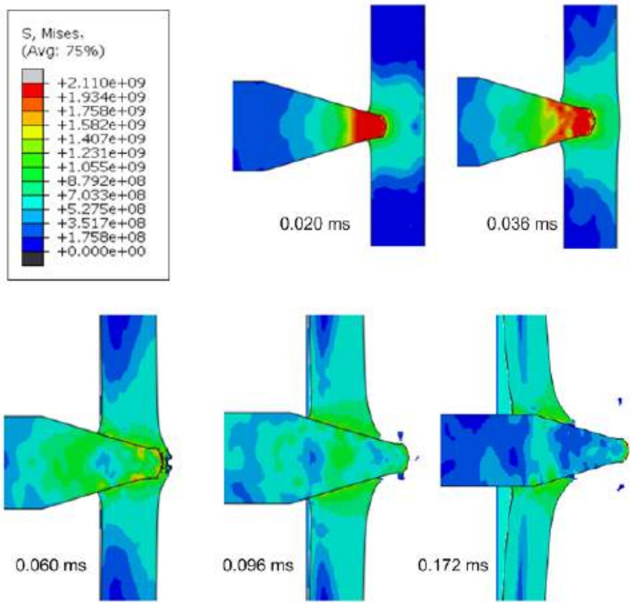

Figure 11.Von Mises stress distribution in [Pa] during the 300 m/s impact of the conical shaped impactor at the 12 mm thick plate.

The residual velocity curves for the conically shaped impactor are displayed in Figure 12. The numerically predicted results are a very good match to the experimental data provided in (Børvik, 2000) for the blunt and conically shaped impactors. The ballistic curves are in this case shifted to the right-hand side of the diagram, indicating that the conical impactor will have a lower perforation ability compared to the blunt impactor. This observation was not expected considering the fact that the realistic projectiles are sharp or conically shaped. However, the explanation for this result can be found in the fact that the sharp or conically shaped impactors have a better perforation performance compared to blunt impactors if the target plate has an increased thickness. The lower perforation performance of the blunt impactors is in this case caused by the disintegration/fragmentation of the impactor as observed in the experimental testing in (Børvik, 2000). Furthermore, the blunt impactors would have a considerably higher drag compared to the conically shaped impactor.

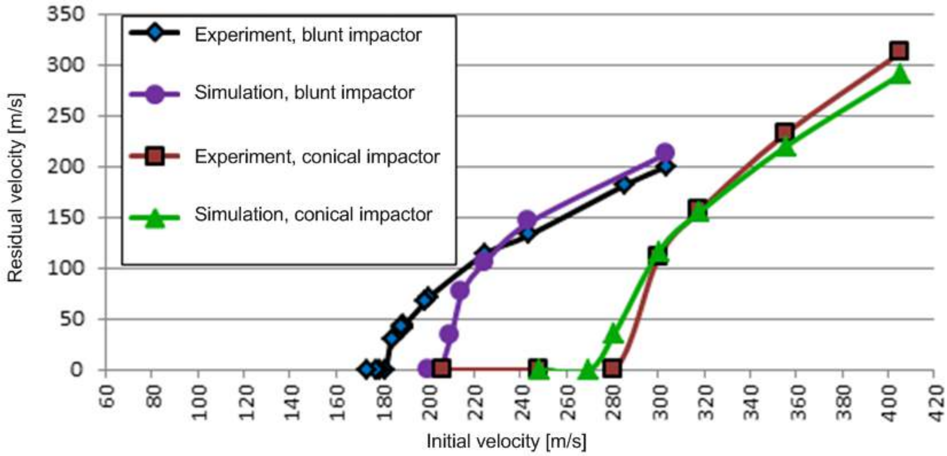

Figure 12.Comparison of ballistic curves for the blunt and conically shaped impactor, 12 mm thick plate.

Figure 13 shows the impact scenarios that have been simulated as to investigate the effect of target plate configuration on the ballistic performance of the plates. The target plate configuration shown in the right-hand side image of Figure 13 is the representation/approximation of realistic armor protection, where various lightweight materials are used to separate the armor plates.

The initial velocity of the conically-shaped impactor in these simulations has been 550 m/s. The average velocity of the nodes at the rear end of the impactor is plotted in Figure 14 for the three analyzed target configurations. Additionally, the results for the homogeneous 12 mm thick plate are also shown in this Figure as to compare these results to the results of the third target plate configuration which consists of two separated 12 mm thick plates.

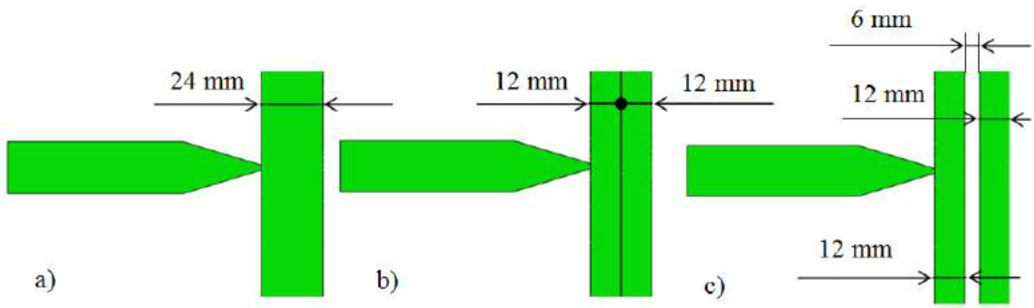

Figure 13.Target plate configurations analyzed in this work: a) homogenous plate b) layered plate c) layered plate with a 6 mm interspace between the plates.

As shown in Figure 14, the 24 mm thick homogeneous plate has the best ballistic protection capability, since the impactor residual velocity is the lowest in this case. This result is closely followed by the target plate with the two plates without interspace, whereas the third target plate configuration has the lowest ballistic protection performance. This is in accordance with the results provided in (Jankowiak, 2013).

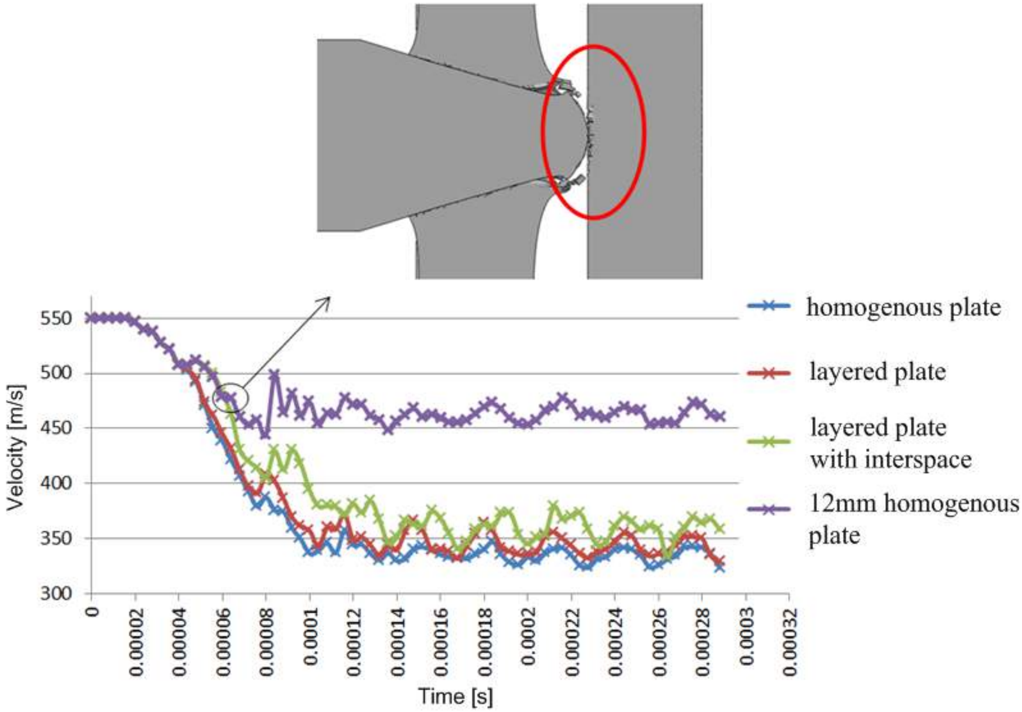

Figure 14.Comparison of impactor velocity during the perforation of the three target plate configurations.

5. Conclusions

This work presents the numerical approach for the modelling of the high velocity perforation of 10 – 24 mm thick steel plates. The exploited numerical approach depicts the preliminary phase of the research in the numerical modeling of advanced armor protection. The methodology is based on the Abaqus/Explicit software as to exploit the built-in capabilities, which are appropriate for the analyzed physical behavior. The implemented finite element model, contact algorithm and material models resulted in the robust and efficient numerical framework for the simulation of the perforation phenomena. Comparison with the experimental data from the literature indicates that the physical behavior of the target plates has been simulated with sufficient accuracy. The characteristic phenomena that occur during the high velocity perforation have been realistically simulated by the numerical framework, as described in Section 4. The future research in this field will be directed towards the more accurate and numerically efficient modeling of advanced armor protection.

6. References

1. Abaqus User's Manual, Version 6.10-1, Dassault Systémes Simulia Corp., Providence, RI.
2. Ali, Y., and A. Riad "Perforation of Thick Plates by High-Speed Projectiles," 13th International Conference on Aerospace Sciences & Aviation Technology, ASAT-13, Cairo, 2009.
3. Arias, A., Rodriguez-Martinez, J., and A. Rusinek, "Numerical simulations of impact behavior of thin steel plates subjected to cylindrical, conical and hemispherical non-deformable projectiles," Engineering Fracture Mechanics, no. 75, 2008.
4. Børvik, T., "Ballistic penetration and perforation of steel plates," NTNU, Trondheim, 2000.
5. He, A., Xie, G., Zhang, H., and X. Wang, "A comparative study on Johnson-Cook, modified Johnson-Cook and Arrhenius-type constitutive models to predict the high temperatureflow stress in 20CrMo alloy steel," Materials and Design, no. 52, 2013.
6. Jankowiak, T., Rusinek, A., and P. Wood, "A numerical analysis of the dynamic behaviour of sheet steel perforated by a conical projectile under ballistic conditions," Finite Elements in Analysis and Design, no. 65, 2013.
7. Johnson, G.R., and W. H. Cook, "A constitutive model and data for metals subjected to large strains, high strain rates and high temperatures," 7th Symposium on ballistics, Hague, 1983.
8. Kiliç, N., and B. Ekici, "Ballistic resistance of high hardness armor steels against 7.62 mm armor piercing ammunition," Materials and Design, no. 44, 2013.
9. Shánĕl, V., and M. Španiel, "Ballistic impact experiments and modelling of sandwich armor for numerical simulations," 37th National Conference on Theoretical and Applied Mechanics (37th NCTAM 2013) &The 1st International Conference on Mechanics (1st ICM), Hsinchu, 2014.